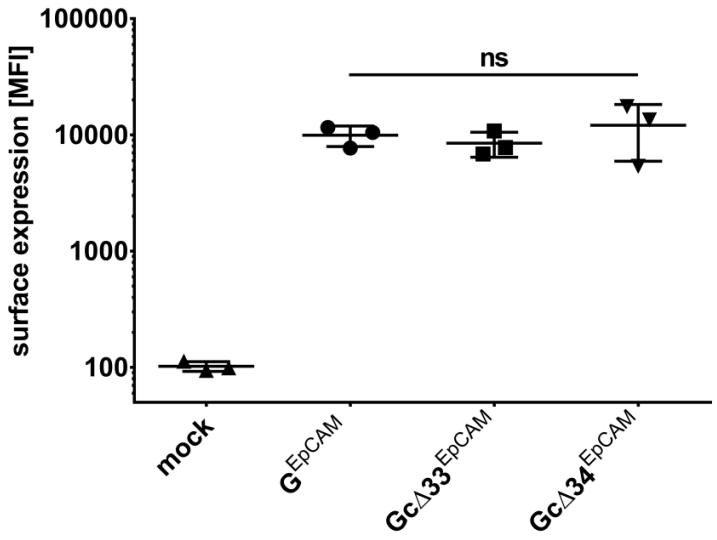

Figure S1: Scatter dot blot of fluorescence intensities of Fig 1C. Mean fluorescence intensities of HEK-293T cells transiently transfected with expression plasmids encoding the indicated EpCAM-displaying cytoplasmic tail truncation variants of G compared to mock transfected cells as determined by flow cytometry. Cells were stained with PE-coupled anti-His antibody (n=3; mean ± standard deviations (SD) are shown; ns, not significant by one-way ANOVA with Tukey's multiple comparisons test).

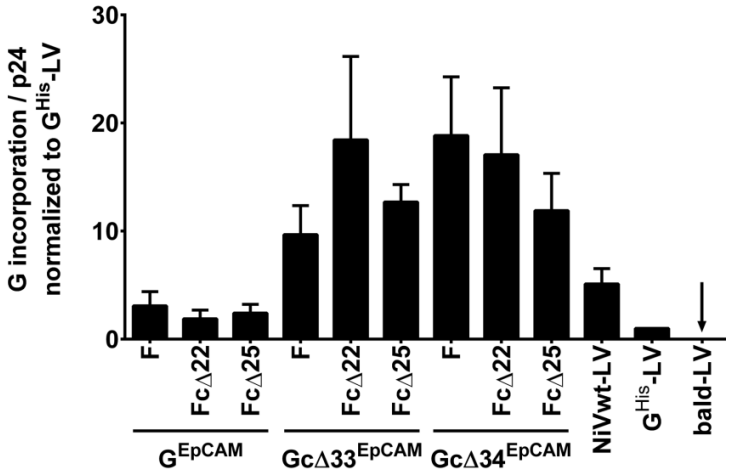

Figure S2: Quantification of Western blot Fig 1D. Western blot analysis of LV particles for incorporation of G^{EpCAM}, $Gc\Delta33^{EpCAM}$, and $Gc\Delta34^{EpCAM}$ and the three different F variants (full length F, FcΔ22 and FcΔ25). $2.5x10^{10}$ particles per sample were applied. NiV-G^{His}/F (G^{His}-LV) and $Gc\Delta34^{His}$/FcΔ22 (NiVwt-LV) pseudotyped LVs as well as concentrated supernatant of mock transfected cells (mock) and concentrated supernatant of cells transfected with the *gag/pol* encoding plasmid pCMVΔR8.9 (bald-LV) served as control. Proteins were detected by chemiluminescense. Chemiluminescense values for the glycoprotein G variants were normalized to those of p24. Values are shown relative to that of G^{His}-LV. Data are mean values obtained from three independently generated vector stocks for each indicated envelope protein combination (n=3; mean ± standard error of the mean (SEM) are shown).

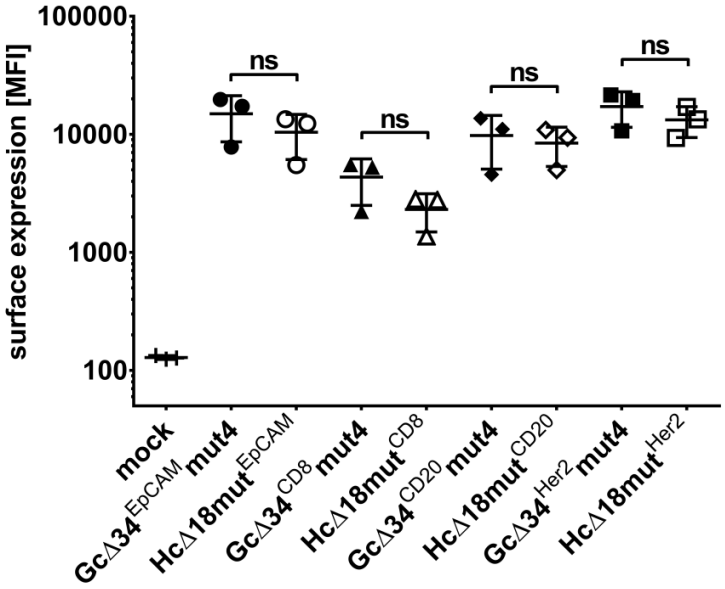

Figure S3: Scatter dot blot of fluorescence intensities of Fig 5A. Mean fluorescence intensities of surface expression of NiV G proteins targeted to four different receptors were compared to those of their corresponding MV H protein counterparts. All expression plasmids encoding the different constructs were transfected into HEK-293T cells. Surface expression was analyzed after 48 hours using a His-tag-specific antibody. Mock transfected cells served as negative control (n=3; mean ± standard deviations (SD) are shown; ns, not significant by unpaired *t*-test).

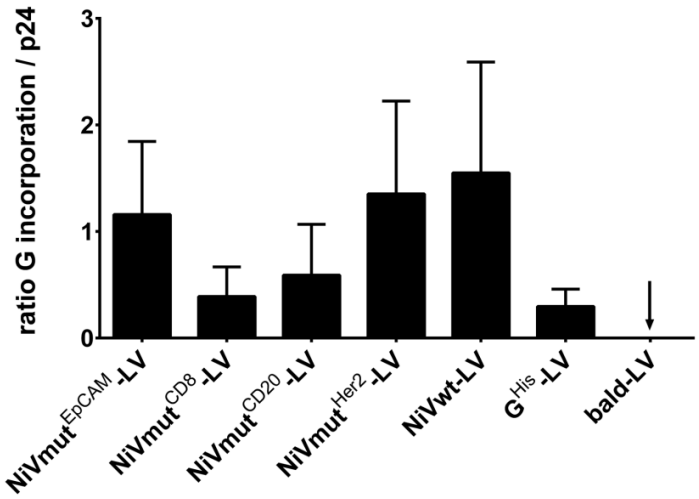

Figure S4: Quantification of Western blot Fig 5B. Three independently generated stocks of NiVmut^{EpCAM}-LV, NiVmut^{CD8}-LV, NiVmut^{CD20}-LV, and NiVmut^{Her2}-LV, were subjected to Western blot analysis applying 2.5x10^{10} particles per sample, respectively. Stocks prepared from mock transfected cells (mock) as well as stocks containing bald particles without glycoproteins (bald-LV) served as controls. In addition, particles pseudotyped with full-length His-tagged G and AU1 tagged F (G^{His}-LV) as well as particles pseudotyped with GcΔ34^{His}/FcΔ22-AU1 (NiVwt-LV) were used. Proteins were detected by chemiluminescense. Chemiluminescense values for the glycoprotein G variants were normalized to those of p24 (n=3; mean ± standard error of the mean (SEM) are shown).

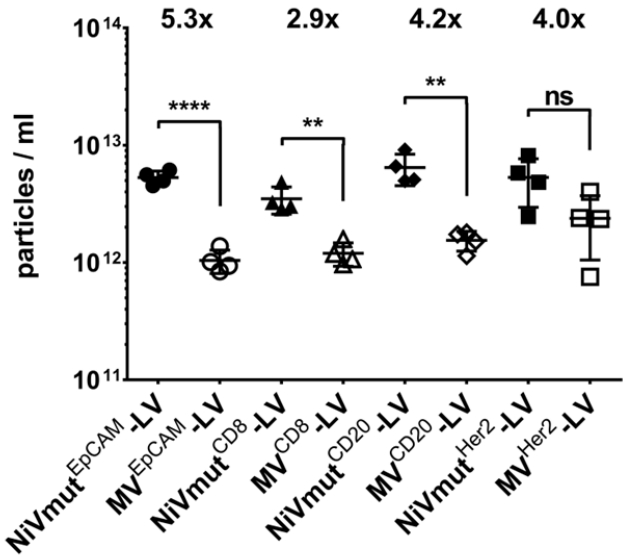

Figure S5: Particle concentration of lentiviral vector stocks shown in Fig 5C. The numbers of physical particles per ml were determined by single nanoparticle tracking analysis (NTA). The fold increase of particle numbers for the NiV-LV based stocks compared to the corresponding MV-LV based stocks are indicated. For each vector type mean values of four independently generated vector stocks are shown (n=4; mean ± standard deviations (SD) are shown; **, P<0.01; ****, P<0.0001; ns, not significant by unpaired *t*-test).

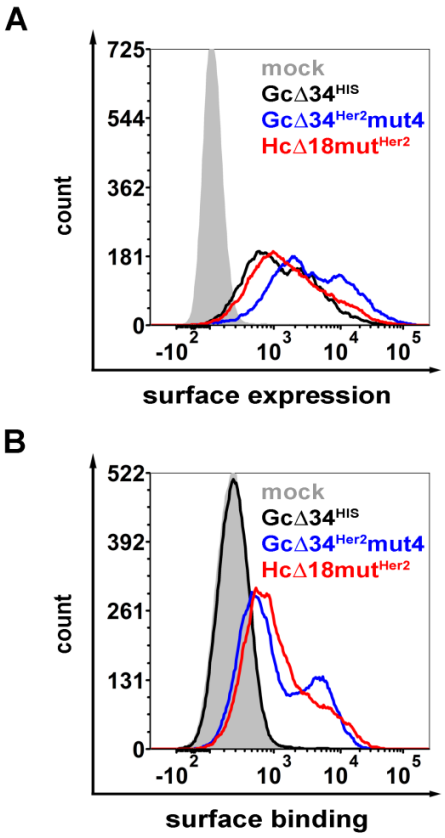

Figure S6: Binding of recombinant Her2/*neu*. (A) Exemplary flow cytometry blot of surface expression of NiV-GcΔ34^{Her2}mut4 (blue line) and HcΔ18mut^{Her2} (red line) in comparison to NiV-GcΔ34^{His} (black line). HEK-293T cells were transiently transfected with plasmids encoding the different glycoproteins compared to mock transfected cells (filled curve) as determined by flow cytometry. Cells were stained with PE coupled anti-His antibody. One representative out of three experiments is shown. (**B**) NiV-GcΔ34^{Her2}mut4 (blue line), HcΔ18mut^{Her2} (red line) and NiV-GcΔ34^{His} (black line) were expressed on HEK-293T cells, incubated for 1 h at 4°C with 1 µg/ml recombinant Fc-Her2/*neu* prior to staining against Fc-tag using FITC coupled anti-Fc antibody. Mock transfected cells (filled curve) served as control. One representative out of three experiments is shown.

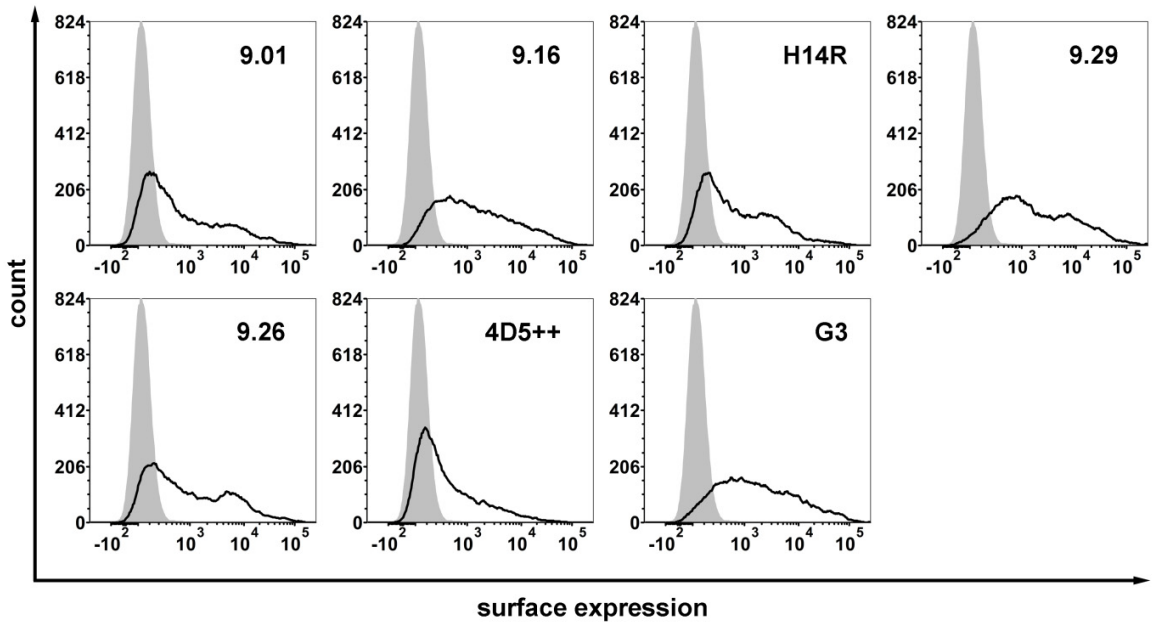

Figure S7: Surface expression of Her2/*neu* DARPin displaying G proteins. Representative flow cytometry plots showing the cell surface expression of GcΔ34^{Her2}mut4 variants fused to the indicated Her2/*neu*-specific DARPins (9.01, 9.16, H14R, 9.29, 9.26, G3) or the scFv 4D5++ after transient transfection of HEK-293T cells with the corresponding expression plasmids (empty curves) compared to mock transfected cells (filled curves). Cells were stained with PE-coupled anti-His antibody.

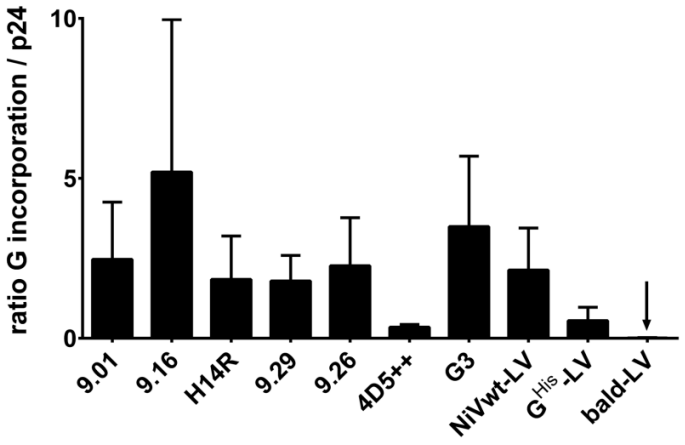

Figure S8: Quantification of LV particle incorporation levels of Her2-targeted G protein variants. The data refer to the exemplary Western blot shown in Fig 8G. Chemiluminescence values for the glycoprotein G variants and those of p24 were quantified from three Western blots and three independently generated vector stocks, respectively. Values for the G variants normalized to those of p24 are shown (n=3; mean ± standard error of the mean (SEM) are shown).

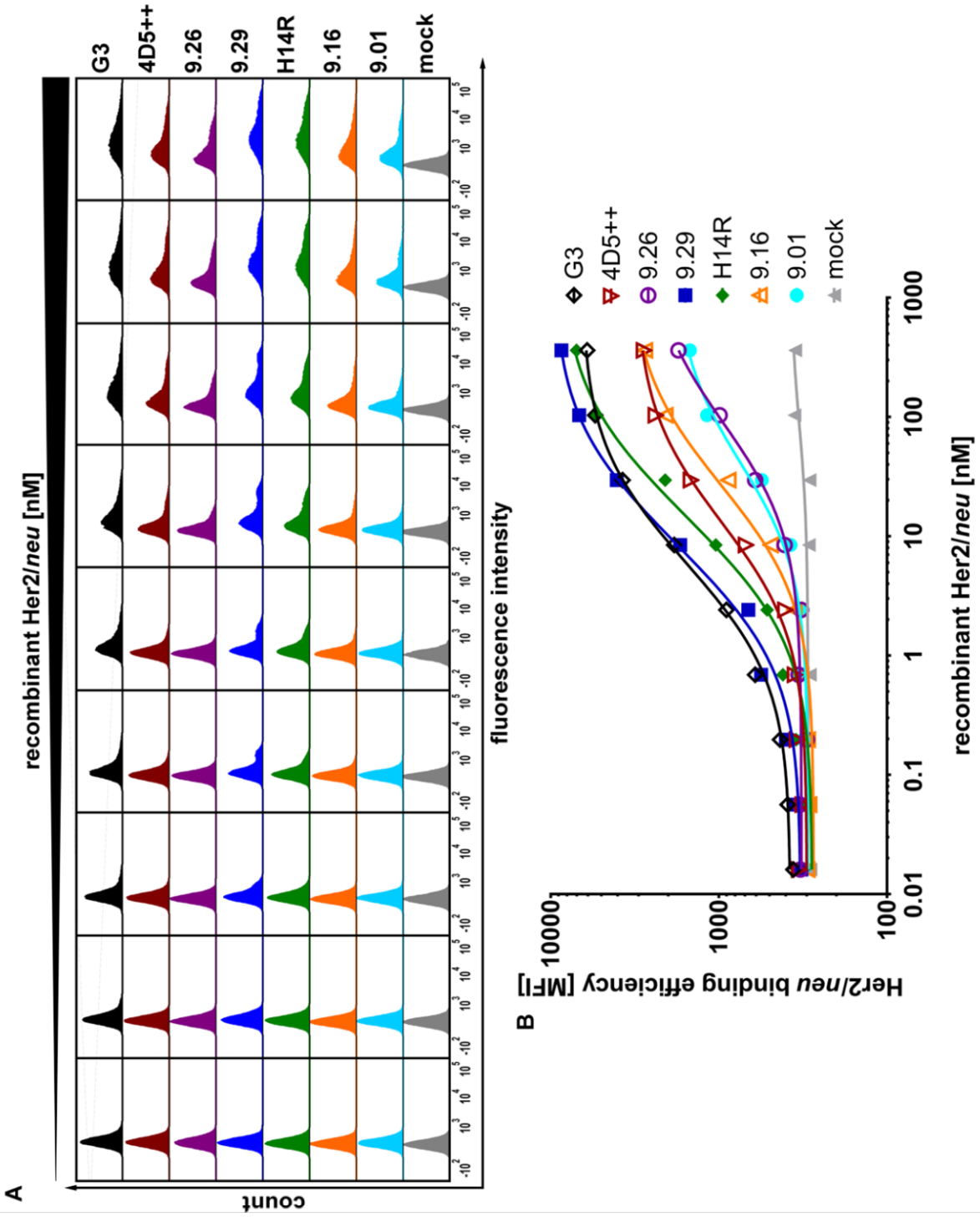

Figure S9: Binding of recombinant Her2/*neu* to Gc∆34^{Her2}mut4 variants. (**A**) Flow cytometry plots obtained after transient transfection of HEK-293T cells with expression plasmids encoding Gc∆34^{Her2}mut4 variants displaying either DARPin G3 (black), 9.26

(purple), 9.29 (blue), H14R (green), 9.16 (orange), 9.01 (cyan), or the scFv 4D5++ (red) and incubation for 1 h at 4°C with increasing molar concentrations of recombinant Fc-Her2/*neu* prior to staining against Fc-tag using FITC coupled anti-Fc antibody. Mock transfected cells were included as control (mock). (**B**) MFIs of the complete cell populations shown in (**A**) are plotted against the concentrations of recombinant Her2/*neu* applied for binding.

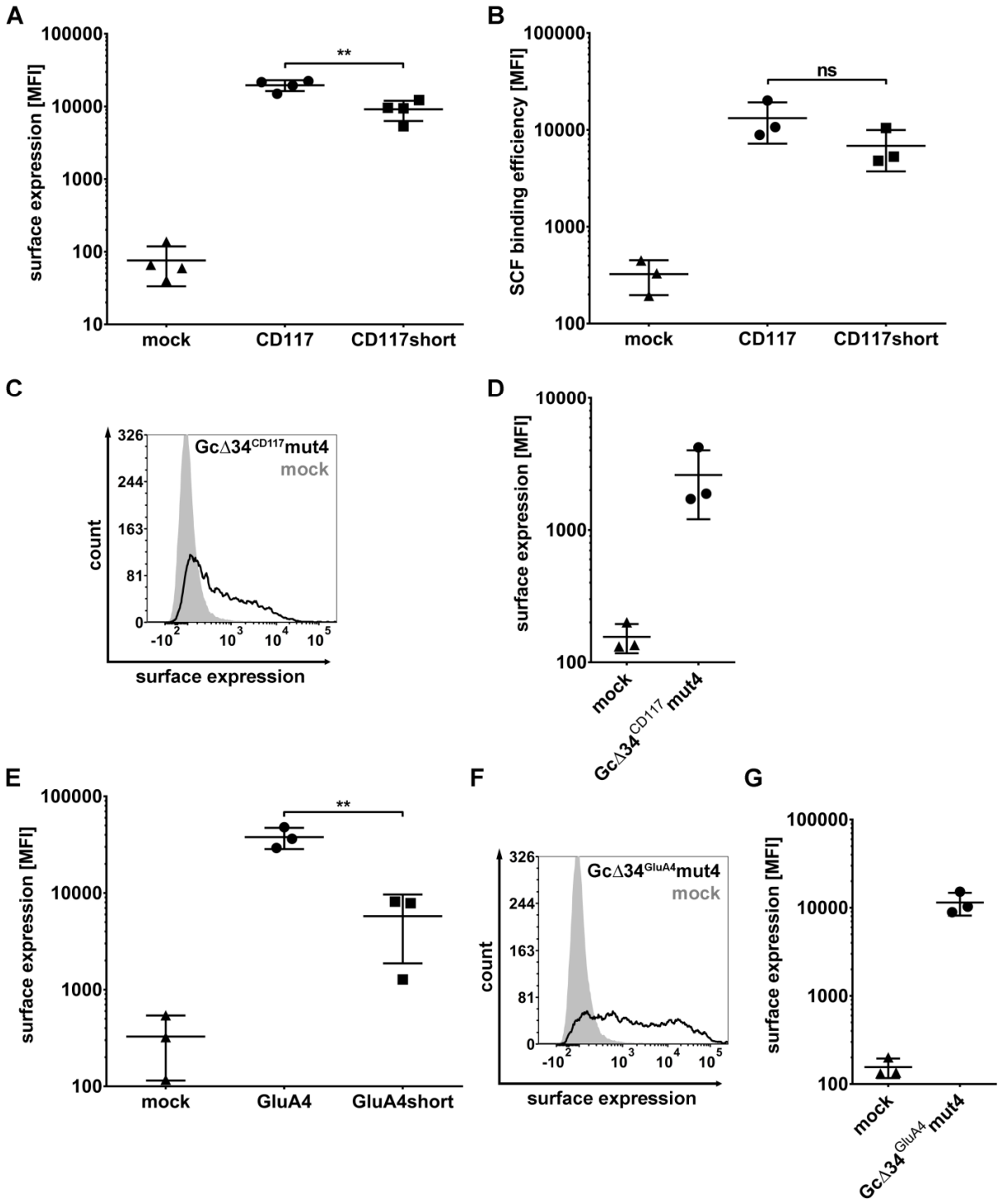

Figure S10: CD117- and GluA4-targeted NiV-LV. (**A**) Scatter dot blot of fluorescence intensities of Fig 9A. Mean fluorescence intensities of surface expression of CD117 and CD117short on HT1080 are shown. Surface expression was analyzed using a CD117-

specific antibody. Parental HT1080 cells served as negative control (mock) (n=4; mean ± standard deviations (SD) are shown; **, P<0.01 by unpaired *t*-test). (**B**) Scatter dot blot of fluorescence intensities of Fig 9C. Mean fluorescence intensities of surface binding of Fc-SCF to HT1080-CD117 and HT1080-CD117short are shown. Surface binding was analyzed using a FITC coupled anti-Fc antibody. Parental HT1080 cells served as negative control (mock) (n=3; mean ± standard deviations (SD) are shown; ns, not significant by unpaired *t*-test). (**C**) Exemplary flow cytometry blot of surface expression of NiV-GcΔ34^{CD117}mut4 (black line). HEK-293T cells were transiently transfected with plasmids encoding the glycoprotein and compared to mock transfected cells (filled curve) as determined by flow cytometry. Cells were stained with PE coupled anti-His antibody. One representative out of three experiments is shown. (**D**) Scatter dot blot of fluorescence intensities in (**C**). Mean fluorescence intensities of surface expression of the CD117-targeted G variant on HEK-293T cells transiently transfected with the corresponding expression plasmid compared to mock transfected cells as determined by flow cytometry. Cells were stained with PE-coupled anti-His antibody (n=3; mean ± standard deviations (SD) are shown). (**E**) Scatter dot blot of fluorescence intensities of Fig 9B. Mean fluorescence intensities of surface expression of GluA4 and GluA4short on HT1080 are shown. Surface expression was analyzed using a myc-tag specific antibody. Parental HT1080 cells served as negative control (mock) (n=3; mean ± standard deviations (SD) are shown; **, P<0.01 by unpaired *t*-test). (**F**) Exemplary flow cytometry blot of surface expression of NiV-GcΔ34^{GluA4}mut4 (black line). HEK-293T cells were transiently transfected with plasmids encoding the glycoprotein and compared to mock transfected cells (filled curve) as determined by flow cytometry. Cells were stained with PE coupled anti-His antibody. One representative out of three experiments is shown. (**G**)

Scatter dot blot of fluorescence intensities in (**F**). Mean fluorescence intensities of surface expression of GluA4-targeted G variant on HEK-293T cells transiently transfected with the corresponding expression plasmid compared to mock transfected cells as determined by flow cytometry. Cells were stained with PE-coupled anti-His antibody (n=3; mean ± standard deviations (SD) are shown).

Table S11: PCR primers for cloning

Name	Sequence (5’ – 3’)
AgeI-DARPin fwd	ATA TAC CGG TGA CCT GGG TAA GAA ACT GCT GGA AG
AgeI-DARPin-G3 fwd	ATA TAC CGG TGA CCT GGG TAA GAA ACT ACT GGA AGC
AgeI-$(G_4S)_3$ fwd	ATA TAC CGG TGG AGG TGG CTC TGG TG
AgeI-NiV-G rev	ATA TAC CGG TGC ACT GCT CGG GGA TC
AgeI-NiV-G(I588) rev	GGT CAC CGG TGC ACT GCT CGG GGA TCT TCA CGG CGA ACA GCT TGG GCC TGG CCA CGT TGT CGC CGG TAT CG
AgeI-scFv-CD20 fwd	ATA TAC CGG TAT GGC TCA GGT TCA GCT GGTC
BamHI-cKIT fwd	ATA TGG ATC CAC CGG TCG CCA CCA TGA GAG GCG CTC G
BamHI-ephrin-B2 fwd	TAT AGG ATC CGC CAC CAT GGC TGT GAG AAG GGA CTC C
BamHI-GluA4 fwd	ATA TGG ATC CAC CGG TCG CCA CCA TGA GGA TTA TTT GCA GG
BsiWI-CD4-TM fwd	ATA TCG TAC GTC GGG ACA GGT CC
cKIT-D3-BsiWI rev	ACC TCG TAC GTA CTA CTT CCA AGG TTG TTG
cKIT-SpeI rev	GGT GTA CTA GTT CAG ACA TCG TCG TGC
GluA4-SpeI rev	CAG TAC TAG TTT ATG GTA GGT CCG ATG
GluA4-ATD-BsiWI rev	GCC GCG TAC GCA TAT CTT GAA TCA AGA C
HIS-DARPin rev	GTG ATG GTG ATG GTG ATG AGA ACC TCT TG
NiV-F fwd	CGC GTT AAT TAA GCC ACC ATG GTA GTT ATA C
NiV-FcΔ22-AU1 rev	GTA CGA GCT CTT AGA TGT ACC TGT ACG TGT CGG TGT TTC TCT TTT TCT CAA C
NiV-FcΔ25-AU1 rev	ATA TGA GCT CTT AGA TGT ACC TGT ACG TGT CCT TTT TCT CAA CAA TGA TAA AAC TGA TAA ATG
NiV-F-AU1 rev	GAT CGA GCT CTT AGA TGT ACC TGT ACG TGT CTG TCC CAA TGT AGT AGA GAT C
NiV-G(E501+W504) fwd	CAA CAC CTG CCC CGC GAT CTG CGC GGA GGG CGT GTA C
NiV-G(E501+W504) rev	GTA CAC GCC CTC CGC GCA GAT CGC GGG GCA GGT GTT G
NiV-G(E501A) fwd	CAA CAC CTG CCC CGC GAT CTG CTG GGA GG
NiV-G(E501A) rev	CCT CCC AGC AGA TCG CGG GGC AGG TGT TG
NiV-G(E533A) fwd	CAA CCA GAC CGC CGC GAA TCC CGT GTT CAC

NiV-G(E533A) rev	GTG AAC ACG GGA TTC GCG GCG GTC TGG TTG
NiV-G(Q530A+E533A) fwd	CTG GAC TCC AAC GCG ACC GCC GCG AAT CCC GTG TTC AC
NiV-G(Q530A+E533A) rev	GTG AAC ACG GGA TTC GCG GCG GTC GCG TTG GAG TCC AG
NiV-G(Q530A) fwd	CTG GAC TCC AAC GCG ACC GCC GAG AAT CCC
NiV-G(Q530A) rev	GGG ATT CTC GGC GGT CGC GTT GGA GTC CAG
NiV-G(W504A) fwd	CGA GAT CTG CGC GGA GGG CGT GTA C
NiV-G(W504A) rev	GTA CAC GCC CTC CGC GCA GAT CTC G
NiV-G(Y389A) fwd	CCA TCA CCA AGT GCC AGG CCA GCA AGC CCG AGA AC
NiV-G(Y389A) rev	GTT CTC GGG CTT GCT GGC CTG GCA CTT GGT GAT GG
NotI-DARPin rev	ATA TGC GGC CGC ATT AAG CTT TTG C
NotI-NiV-G rev	ATA TGC GGC CGC GGT GCA CTG CTC GGG GAT CTT CAC
NotI-scFv-CD20rev	ATA TGC GGC CGC CTT CAG CTC CAG CTT GGT CCC AGC AC
PacI-NiV-GcΔ33	GCA CTT AAT TAA GCC ACC ATG ATC AAG AAG ATC AAC GAG GGC CTG CTG
PacI-NiV-GcΔ34	GCA CTT AAT TAA GCC ACC ATG AAG AAG ATC AAC GAG GGC CTG CTG
SacI-NiV-FcΔ22	GGC CGA GCT CTT AGG TGT TTC TCT TTT TCT CAA CAA TG
SacI-NiV-FcΔ25	GGC CGA GCT CTT ACT TTT TCT CAA CAA TGA TAA AAC TGA TAA ATG
SacI-NiV-G rev	ATA TGA GCT CTC AGG TGC ACT GCT CGG GGA TC
SpeI-CD4-TM rev	GCC GAC TAG TTC AAA TGG GGC TAC ATG
SpeI-ephrin-B2 rev	ATA TAC TAG TTT AGA CCT TGT AGT AAA TGT TCG CCG GGC TC